Pentapod Nanostructures

DOI: 10.1002/anie.201002546

Facile Synthesis of Five-fold Twinned, Starfish-like Rhodium Nanocrystals by Eliminating Oxidative Etching with a Chloride-Free Precursor**

Hui Zhang, Xiaohu Xia, Weiyang Li, Jie Zeng, Yunqian Dai, Deren Yang, and Younan Xia**

Rhodium is widely used as a catalyst in a rich variety of reactions such as hydrogenation, hydroformylation, hydrocarbonylation, CO oxidation, and hydrogen generation.[1] It is also of great interest for potential application in surface-enhanced Raman scattering (SERS).[2] In recent years, controlling the size and shape of Rh nanocrystals has attracted extensive attention because these two parameters allow one to tailor their intrinsic properties and thus enhancing their performance in various applications.[3] There has been some great success in using micelles, dendrimers, and other types of soft templates to reduce the size of Rh nanocrystals and thus increase their catalytic activity.[4] However, in comparison with other noble metals such as Au, Ag, Pt, and Pd, there are only a few reports on the synthesis of Rh nanocrystals with well-defined and controllable shapes or morphologies. So far, only single-crystal Rh nanocrystals such as cubes, octahedrons, tetrahedron, or multipods have been reported. For example, the Tilley and Somorjai groups reported the syntheses of Rh nanocrystals in the form of tripods, tetrapods, cubes, horns, and cubooctahedrons through seed-mediated growth by reducing $RhCl_3$ with a polyol under Ar protection.[5] When trimethyl(tetradecyl)-ammonium bromide (TTAB) was employed as a capping agent, relatively uniform, sub-10 nm Rh nanocubes have also been obtained.[6] In a related study, we reported a polyol process for synthesizing Rh tripods using Na_3RhCl_6 as a precursor under Ar protection.[7] The Rh tripods exhibited interesting SERS properties because the electromagnetic field could be greatly enhanced at the tips of the tripod nanostructures. Interestingly, no twinned Rh nanocrystal has ever been reported with a reasonable yield. This result can be attributed to the fact that either $RhCl_3$ or Na_3RhCl_6 has been employed as a precursor to the metal and it is impossible to completely eliminate oxidative etching by simply bubbling an inert gas through the reaction system.[5–7]

It is worth pointing out that $RhCl_3$ and Na_3RhCl_6 are not good precursors for synthesizing Rh nanocrystals because the Cl^- ions released from the precursors can combine with the O_2 from air to cause oxidative etching during both the nucleation and growth processes.[8] As shown for a number of noble-metal systems, the etching process can cause size polydispersity for the final nanocrystals as etching (like the corrosion of a metal piece) tends to occur in a non-uniform pattern.[9] The etching can also make it very difficult to generate nanocrystals with a twinned structure as the twin defects are highly susceptible to oxidation and dissolution.[10] Although the oxidative etching can be blocked to some extent by protection with an inert gas or through the use of an antioxidant capping agent (e.g., citrate ions or citric acid),[11] it will be a great advantage if we can completely eliminate it by choosing a proper precursor that does not contain the necessary ligand required for oxidative etching.

Herein, we report a facile synthesis of starfish-like Rh nanocrystals with five twined arms in a polyol system as well as their excellent performance as substrates for SERS. The nanocrystal grows from the corners of a five-fold twinned, decahedral seed. The idea is based upon our previous study which showed that Rh tripods could only prevail when oxygen was excluded from a reaction system to block oxidative etching.[7] In this study, we completely eliminate the oxidative etching by using $[\{(CF_3COO)_2Rh\}_2]$ instead of Na_3RhCl_6 as a precursor. Due to the exclusion of Cl^- ions from the reaction system, five-fold twinned Rh nanocrystals with five branched arms could be obtained in high yields.

In a typical synthesis, $[\{(CF_3COO)_2Rh\}_2]$ and poly(vinyl pyrrolidone) (PVP) were dissolved separately in ethylene glycol (EG), and these two solutions were then injected simultaneously using a syringe pump into EG held at a specific temperature. The color of the solution immediately turned from deep blue to black, indicating the formation of Rh nanocrystals due to the reduction of $[\{(CF_3COO)_2Rh\}_2]$ by EG (see Experimental Section for details). Figure 1a and b shows transmission electron microscopy (TEM) images of a typical sample prepared at 180 °C for 6 h. These TEM images clearly show that most of the Rh nanocrystals consisted of five arms (like a starfish), with an angle of 72° between adjacent ones. The Rh arms were 4–10 nm in width and 6–12 nm in

[*] Dr. H. Zhang, X. Xia, W. Li, J. Zeng, Y. Dai, Prof. Y. Xia
Department of Biomedical Engineering, Washington University
Saint Louis, MO 63130 (USA)
E-mail: xia@biomed.wustl.edu
Dr. H. Zhang, Prof. D. Yang
State Key Laboratory of Silicon Materials, and Department of Materials Science and Engineering, Zhejiang University
Hangzhou, Zhejiang 310027 (People's Republic of China)
E-mail: msezhanghui@zju.edu.cn

[**] This work was supported in part by a DOE subcontract from the University of Delaware (DE-FG02-03 ER15468) and startup funds from Washington University in St. Louis. As a visiting scholar from Zhejiang University, H.Z. was also partially supported by the "New Star Program" of Zhejiang University. Part of the work was performed at the Nano Research Facility (NRF), a member of the National Nanotechnology Infrastructure Network (NNIN), which is supported by the NSF under award ECS-0335765.

Supporting information for this article is available on the WWW under http://dx.doi.org/10.1002/anie.201002546.

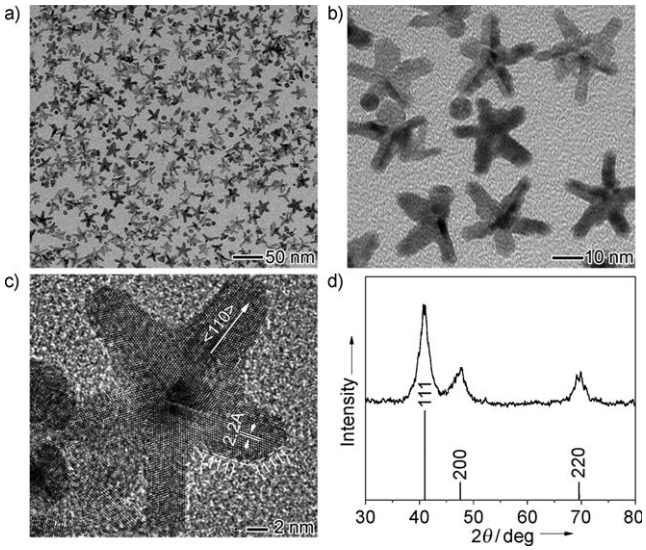

Figure 1. a, b) TEM images, c) high-resolution TEM image, and d) XRD pattern of a typical sample of starfish-like Rh nanocrystals prepared using polyol reduction at 180 °C for 6 h.

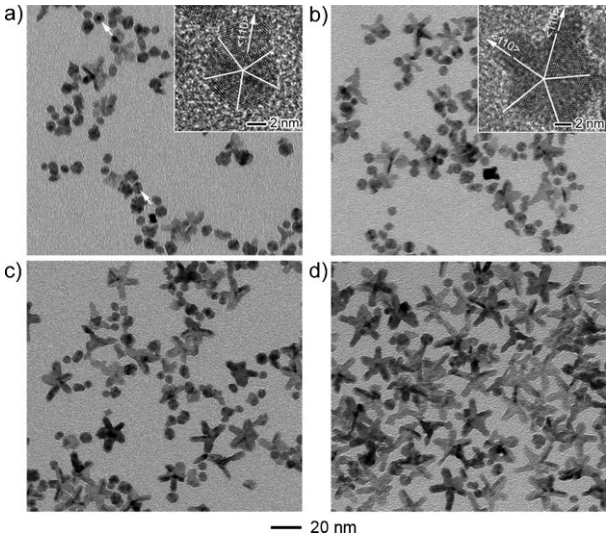

Figure 2. TEM images of Rh nanocrystals obtained at 180 °C after injection of precursor for different periods of time: a) 0; b) 1 min; c) 10 min; and d) 20 h. The insets show high-resolution TEM images taken from the corresponding samples.

length, whereas the overall size of the nanocrystal was on the order of 30 nm. A small number of icosahedral Rh nanocrystals of 6–10 nm in size also coexisted with the starfish-like nanocrystals in the final product (see Supporting Information for structural characterization, Figure S1). Figure 1c shows high-resolution TEM image of an individual starfish-like Rh nanocrystal, where periodic lattice fringes could be clearly resolved. The lattice spacing of each group of parallel fringes was about 0.22 nm, corresponding to the {111} planes. Further analysis indicates that the arms grew from the five corners of a five-fold twinned, decahedral core along the $<110>$ direction to generate a starfish-like structure, which is considerably different from the growth behavior of other noble metals such as Ag. In the case of Ag, a decahedral seed would grow into a five-fold twinned nanorod and then a nanowire, rather than a starfish-like nanocrystal probably due to preferential stabilization of the newly formed {100} side faces by PVP through selective chemisorption.[12] We believe that the different growth behaviors for Rh and Ag decahedral seeds are most likely induced by the different chemisorption capabilities of PVP on the {100} faces of these two noble metals. Figure 1d shows an X-ray diffraction (XRD) pattern of the starfish-like Rh nanocrystals. All the diffraction peaks could be indexed to the face-centered cubic Rh (JCPDS No.001-1214). The broadening of the diffraction peaks can be attributed to the relatively small sizes of the Rh arms in the nanocrystals.[13]

In order to clarify the formation mechanism of the starfish-like Rh nanocrystals, a series of TEM images were taken from the samples prepared at different reaction times, as shown in Figure 2. In the initial stage of the reaction (Figure 2a), nanocrystals with sizes of several nanometers were formed. Analysis by high-resolution TEM imaging (see inset of Figure 2a for a typical example) revealed that the sample was dominated by Rh decahedrons, together with some icosahedrons as marked by arrows. We believe that the use of a high temperature (180 °C) and the absence of Cl^- ions were responsible for the formation of decahedral and icosahedral nanocrystals because they are supposed to be the most stable species for a face-centered cubic crystal when the reduction is conducted under thermodynamic control.[14] The UV/Vis spectra (Figure S2) taken from the solution at different stages of the reaction indicate that the precursor was consumed in 1 min due to rapid reduction and the monomer was quickly depleted in the solution, confirming that the synthesis was under a thermodynamic control.[15] Tiny tips also started to grow from the corners of some decahedrons along the $\langle 110 \rangle$ direction. As the reaction was continued (Figure 2b), more and longer tips were observed to protrude from the corners of the decahedral seeds, and some small starfish-like nanocrystals could be clearly resolved. Figure 2a and b clearly show that the growth of different arms, even those from the same seed, might take place at different time points, resulting in different lengths for the arms in the starfish-like nanocrystals. Since the precursor was completely depleted in 1 min, the growth of the starfish-like nanocrystals was mainly driven by Ostwald ripening at the expense of icosahedral nanocrystals (as well as some small Rh clusters that might also existed in the solution). This growth mechanism was consistent with the fact that icosahedrons are usually stable at small sizes, and decahedrons at medium sizes.[16] As a result, the growth rate of the starfish-like nanocrystals was strongly reduced in comparison to the formation of the decahedral or icosahedral nanocrystals in the initial stage. Even after 10 min of reaction, only a few starfish-like nanocrystals were formed, as shown in Figure 2c. With extension of the reaction time to 6 h, most of the decahedral Rh nanocrystals had been transformed into starfish-like nanocrystals. Further extension to 20 h (Figure 2d) did not result in any obvious morphological change, indicating that the starfish-like Rh nanocrystals were highly stable in EG at an elevated temperature due to the exclusion of oxidative etching.

The aforementioned results indicate that the formation of the starfish-like Rh nanocrystals was thermodynamically controlled in the initial stage. As a parameter critical for the control of reduction rate, the reaction temperature should play an important role. Figure 3 shows TEM images of the

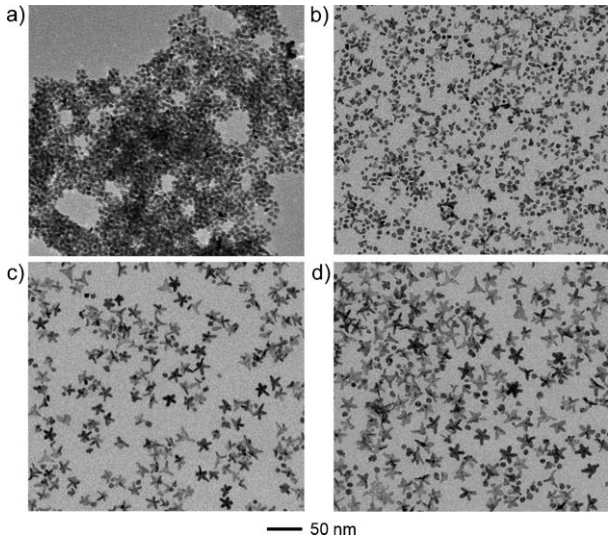

Figure 3. TEM images of Rh nanocrystals prepared at different temperatures for 6 h: a) 120, b) 160, c) 170, and d) 190 °C.

products obtained at other temperatures. It is clear that only nanoparticles with sizes less than 10 nm were formed when the temperature was set to 120 °C (Figure 3a). In contrast, an increase of the temperature to 160 °C (Figure 3b) led to the formation of the starfish-like Rh nanocrystals. Significantly, the amount of the starfish-like nanocrystals was increased as the reaction temperature was further increased to 170 and 190 °C, as shown in Figure 3c and d. These temperature-dependent experiments further confirmed that the growth of the starfish-like Rh nanocrystals was a result of thermodynamically controlled reduction.

We also systematically investigated the effect of the precursor type on the morphology of the Rh nanocrystals. In the presence of Cl^- ions, for example, with the use of Na_3RhCl_6 (Figure 4a) or $[\{Rh(CF_3COO)_2\}_2]$ + HCl (1:1 molar ratio, Figure 4b) as a precursor, both irregularly shaped Rh nanocrystals and tripods were obtained due to oxidative etching, which was in agreement with our previous report.[7] In the absence of Cl^-, for example, with $[\{Rh(CH_3COO)_2\}_2]$ (Figure 4c) or $[\{Rh(CF_3COO)_2\}_2]$ + citric acid (Figure 4d) as the precursor, twinned nanocrystals containing at least one twin defect were obtained due to the elimination of oxidative etching. These twinned seeds could further evolve into bipyramids, decahedrons, or icosahedrons under thermodynamic control. The slight difference between the ligands in $[\{Rh(CF_3COO)_2\}_2]$ and $[\{Rh(CH_3COO)_2\}_2]$ led to subsequent evolution of the decahedral seeds into the starfish-like nanocrystals or other forms. Although the exact mechanism is yet to be elucidated, the different reduction rates associated with these two precursors might be responsible for the different pathways. Moreover, in agreement with previous

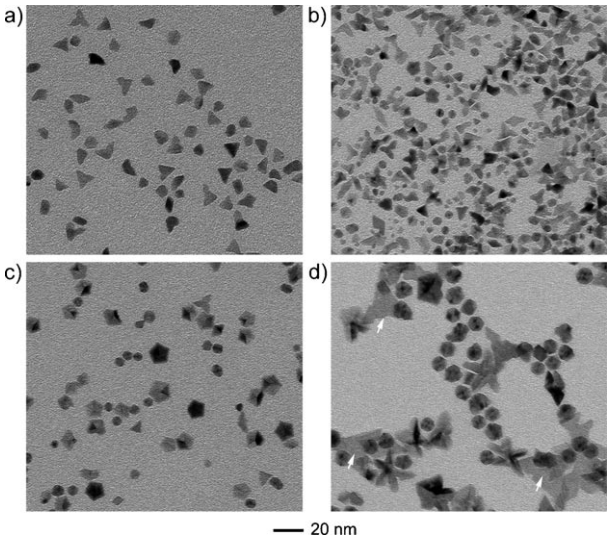

Figure 4. TEM images of Rh nanocrystals prepared at 180 °C for 6 h using a) Na_3RhCl_6, b) $[\{Rh(CF_3COO)_2\}_2]$ + HCl, c) $[\{Rh(CH_3COO)_2\}_2]$, d) $[\{Rh(CF_3COO)_2\}_2]$ + citric acid as precursor.

studies, some Rh nanoplates were formed in the presence of citric acid, as shown in Figure 4d (indicated by arrows), due to their strong binding to the {111} facets.[17] As a coordination ligand, citric acid could also decrease the reduction rate of the precursor by altering the equilibrium potential of divalent Rh,[18] and thus strongly inhibiting the formation of the starfish-like Rh nanocrystals.

The branched morphology intrinsic to the starfish-like Rh nanocrystals make them attractive for use as SERS substrates because in many cases branching can lead to larger surface areas and thus stronger SERS signals.[19] Figure 5 compares the SERS activities of Rh thin films consisting of three types of Rh nanocrystals with different morphologies: a) the starfish-like nanocrystals (Figure 1a), b) the embryonic Rh

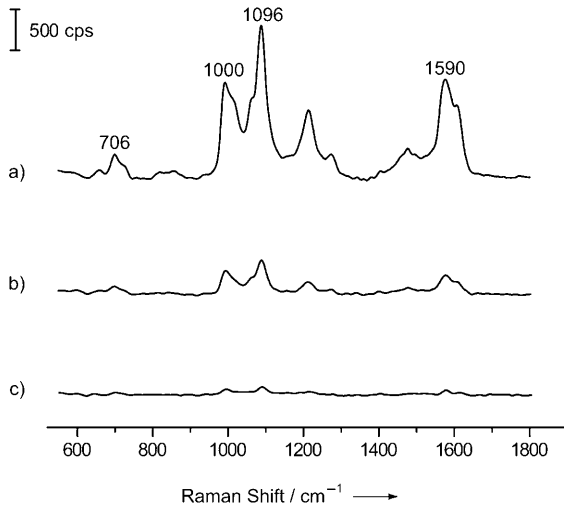

Figure 5. SERS spectra (cps = counts per second) of 4-mercaptopyridine on films of Rh nanocrystals: a) starfish-like Rh nanocrystals (see Figure 1a), b) embryonic Rh multipods (see Figure 4a), and c) spherical Rh nanocrystals (see Figure 3a).

tripods (Figure 4a), and c) the spherical nanocrystals (Figure 3a). We chose 4-mercaptopyridine (4-MP) as a probe molecule because it has a large Raman scattering cross section[20] and has been well established.[21] From the films of Rh nanocrystals that had been modified with 4-MP, it was found that the starfish-like nanocrystals gave the strongest SERS signal with an enhancement of 5 and 20 times stronger than that for the embryonic tripods and spherical nanocrystals, respectively. These results suggest a trend of stronger SERS signal with sharper morphological features on the Rh nanocrystals. Recent studies have shown that metal nanocrystals with sharp corners or edges were especially SERS active since greater field enhancements are observed near the sharpest surface features.[22] This phenomenon was also observed in our previous work, in which the Rh multipods with higher aspect ratios exhibited stronger SERS activities.[7] The SERS results shown here are purely qualitative and exact quantitative analysis for detecting small molecules needs further exploration.

In summary, we have demonstrated a facile polyol approach to the synthesis of starfish-like Rh nanocrystals by replacing the conventional $RhCl_3$ or Na_3RhCl_6 precursor with $[\{Rh(CF_3COO)_2\}_2]$ to completely eliminate oxidative etching. Under thermodynamically controlled conditions, decahedral Rh nanocrystals were initially formed, and then arms gradually protruded from the five corners of the decahedral nanocrystals along the $\langle 110 \rangle$ direction to form the starfish-like Rh nanocrystals, as driven by Ostwald ripening at the expense of icosahedral nanocrystals. The growth parameters such as temperature and precursor type both play important roles in controlling the morphology of the product. The as-prepared starfish-like Rh nanocrystals gave a 5 and 20 times signal enhancement as SERS substrate in comparison to embryonic Rh tripods and spherical Rh nanocrystals due to the sharper morphological features. Considering their superior SERS activities, it is anticipated that the starfish-like Rh nanocrystals presented here may be a promising candidate for the in situ monitoring of catalytic reactions.[23]

Experimental Section

Synthesis of starfish-like Rh nanocrystals: In a typical synthesis, 7 mL of ethylene glycol (EG; J. T. Baker, 9300-01) was placed in a three-neck flask (equipped with a reflux condenser and a magnetic Teflon-coated stirring bar), preheated in air at 110 °C for 2 h, and then ramped to the designated temperature (120, 160, 170, 180, or 190 °C). Meanwhile, 0.01 mmol of rhodium(II) trifluoroacetate dimer ($[\{Rh(CF_3COO)_2\}_2]$, Aldrich, 399191–250 mg) and 0.3 mmol of poly(vinyl pyrrolidone) (PVP; $M_W \approx 55\,000$, Aldrich, 856568–100 g) were separately dissolved in 2 mL of EG at room temperature. These two solutions were then injected simultaneously into the flask through a syringe pump at a rate of 2 mL min^{-1}. Heating of the reaction at the desired temperature was continued for 6 h. In order to clarify the growth mechanism of the starfish-like Rh nanocrystals, a series of samples were taken over the course of each synthesis with a glass pipet. The product was collected by centrifugation and washed with acetone and ethanol several times to remove EG and excess PVP.

Characterizations: The as-obtained samples were characterized by transmission electron microscopy (TEM), powder X-ray diffraction (XRD), and UV/Vis spectroscopy. TEM samples were prepared by placing a drop of the final product (suspended in water) on a carbon-coated copper grid and drying under ambient conditions. TEM imaging was performed using a Phillips CM100 microscope operated at 120 kV. High-resolution HRTEM images were obtained using a JEOL 2100F operated at 200 kV. XRD analysis was performed on Rigaku Geigerflex D-MAX/A Diffractometer using $Cu_{K\alpha}$ radiation. The UV/Vis spectra were recorded with a Cary 50 spectrometer (Varian) using a quartz cuvette with an optical path length of 1 cm. The substrate for SERS was prepared by drying a 5 mL aliquot of the final product on a 50 nm thick Au film supported on a Si wafer. The sample was then incubated in an aqueous solution of 4-mercaptopyridine (5 mM) for 1 h, rinsed with deionized water, and dried in air. The SERS spectra were recorded using a Renishaw inVia confocal Raman spectrometer coupled to a Leica microscope with 50× objective (N.A. = 0.90) in backscattering configuration. The 785 nm excitation (8 mW at the sample) was from a semiconductor diode laser and used with a holographic notchfilter having a grating of 1200 lines per millimeter. The backscattered Raman signals were collected on a thermoelectrically cooled (−60 °C) CCD detector. The scattering spectra were recorded in the range of 550–1800 cm^{-1}, and collected after 60 s of accumulation in one acquisition. Each SERS spectrum was subtracted from the background line that was taken from the clean Au film. OriginLab software (Northampton, MA, USA) was used for SERS spectra baseline-correction. For the baseline correction, a fourth order polynomial function was used to fit and subtract the raw Raman spectrum. The spectra were then smoothed by adjacent averaging at an average number of 4.

Received: April 28, 2010
Published online: June 23, 2010

Keywords: polyol approach · rhodium · SERS · starfish-like nanostructures

[1] a) K. H. Park, K. Jang, H. J. Kim, S. U. Son, *Angew. Chem.* **2007**, *119*, 1170; *Angew. Chem. Int. Ed.* **2007**, *46*, 1152; b) N. R. Shiju, V. V. Guliants, *Appl. Catal. A* **2009**, *356*, 1; c) F. Ungvary, *Coord. Chem. Rev.* **2007**, *251*, 2087; d) M. E. Halttunen, M. K. Niemela, A. O. I. Krause, A. I. Vuori, *Appl. Catal. A* **1999**, *182*, 115; e) M. E. Grass, Y. W. Zhang, D. R. Butcher, J. Y. Park, Y. M. Li, H. Bluhm, K. M. Bratlie, T. F. Zhang, G. A. Somorjai, *Angew. Chem.* **2008**, *120*, 9025; *Angew. Chem. Int. Ed.* **2008**, *47*, 8893; f) F. M. Leibsle, P. W. Murray, S. M. Francis, G. Thornton, M. Bowker, *Nature* **1993**, *363*, 706.

[2] a) M. Moskovits, *J. Raman Spectrosc.* **2005**, *36*, 485; b) R. S. Golightly, W. E. Doering, M. J. Natan, *ACS Nano* **2009**, *3*, 2859; c) X. M. Lin, Y. Cui, Y. H. Xu, B. Ren, Z. Q. Tian, *Anal. Bioanal. Chem.* **2009**, *394*, 1729; d) Z. Q. Tian, Z. L. Yang, B. Ren, J. F. Li, Y. Zhang, X. F. Lin, J. W. Hu, D. Y. Wu, *Faraday Discuss.* **2006**, *132*, 159; e) Z. Q. Tian, B. Ren, D. Y. Wu, *J. Phys. Chem. B* **2002**, *106*, 9463.

[3] a) T. S. Ahmadi, Z. L. Wang, T. C. Green, A. Henglein, M. A. El-Sayed, *Science* **1996**, *272*, 1924; b) Y. N. Xia, P. D. Yang, Y. G. Sun, Y. Y. Wu, B. Mayers, B. Gates, Y. D. Yin, F. Kim, H. Q. Yan, *Adv. Mater.* **2003**, *15*, 353.

[4] a) W. Huang, J. N. Kuhn, C. K. Tsung, Y. W. Zhang, S. E. Habas, P. D. Yang, G. A. Somorjai, *Nano Lett.* **2008**, *8*, 2027; b) J. D. Hoefelmeyer, H. J. Liu, G. A. Somorjai, T. D. Tilley, *J. Colloid Interface Sci.* **2007**, *309*, 86.

[5] a) J. D. Hoefelmeyer, K. Niesz, G. A. Somorjai, T. D. Tilley, *Nano Lett.* **2005**, *5*, 435; b) S. M. Humphrey, M. E. Grass, S. E. Habas, K. Niesz, G. A. Somorjai, T. D. Tilley, *Nano Lett.* **2007**, *7*, 785.

[6] Y. W. Zhang, M. E. Grass, J. N. Kuhn, F. Tao, S. E. Habas, W. Y. Huang, P. D. Yang, G. A. Somorjai, *J. Am. Chem. Soc.* **2008**, *130*, 5868.

[7] N. Zettsu, J. M. McLellan, B. Wiley, Y. D. Yin, Z. Y. Li, Y. N. Xia, *Angew. Chem.* **2006**, *118*, 1310; *Angew. Chem. Int. Ed.* **2006**, *45*, 1288.
[8] Y. N. Xia, Y. J. Xiong, B. K. Lim, S. E. Skrabalak, *Angew. Chem.* **2009**, *121*, 62; *Angew. Chem. Int. Ed.* **2009**, *48*, 60.
[9] a) M. Stratmann, M. Rohwerder, *Nature* **2001**, *410*, 420; b) G. T. Burstein, *Nature* **1991**, *350*, 188.
[10] a) Y. J. Xiong, J. Y. Chen, B. Wiley, Y. N. Xia, Y. D. Yin, Z. Y. Li, *Nano Lett.* **2005**, *5*, 1237; B. K. Lim, M. J. Jiang, J. Tao, P. H. C. Camargo, Y. M. Zhu, Y. N. Xia, *Adv. Funct. Mater.* **2009**, *19*, 189.
[11] a) Y. J. Xiong, J. Y. Chen, B. Wiley, Y. N. Xia, *J. Am. Chem. Soc.* **2005**, *127*, 7332; b) Y. J. Xiong, J. M. McLellan, Y. D. Yin, Y. N. Xia, *Angew. Chem.* **2007**, *119*, 804; *Angew. Chem. Int. Ed.* **2007**, *46*, 790.
[12] Y. G. Sun, Y. N. Xia, *Nano Lett.* **2003**, *3*, 955.
[13] I. S. Park, M. S. Kwon, N. Kim, J. S. Lee, K. Y. Kang, J. Park, *Chem. Commun.* **2005**, 5667.
[14] Y. J. Xiong, Y. N. Xia, *Adv. Mater.* **2007**, *19*, 3385.
[15] Z. A. Peng, X. G. Peng, *J. Am. Chem. Soc.* **2002**, *124*, 3343.
[16] a) F. Baletto, C. Mottet, R. Ferrando, *Phys. Rev. B* **2001**, *63*, 155408; b) F. Baletto, R. Ferrando, *Rev. Mod. Phys.* **2005**, *77*, 371.
[17] Y. G. Sun, B. Mayers, Y. N. Xia, *Nano Lett.* **2003**, *3*, 675.
[18] S. H. Y. Lo, T. Y. Chen, Y. Y. Wang, C. C. Wan, J. F. Lee, T. L. Lin, *J. Phys. Chem. C* **2007**, *111*, 12873.
[19] C. J. Orendorff, A. Gole, T. K. Sau, C. J. Murphy, *Anal. Chem.* **2005**, *77*, 3261.
[20] W. B. Cai, B. Ren, X. Q. Li, C. X. She, F. M. Liu, X. W. Cai, Z. Q. Tian, *Surf. Sci.* **1998**, *406*, 9.
[21] Z. J. Wang, S. L. Pan, T. D. Krauss, H. Du, L. J. Rothberg, *Proc. Natl. Acad. Sci. USA* **2003**, *100*, 8638.
[22] G. C. Schatz, *Acc. Chem. Res.* **1984**, *17*, 370.
[23] R. Gómez, J. M. Perez, J. S. Gullon, V. Montiel, A. Aldaz, *J. Phys. Chem. B* **2004**, *108*, 9943.

